Chemistry & Biology 13, 839–847, August 2006 ©2006 Elsevier Ltd All rights reserved DOI 10.1016/j.chembiol.2006.06.008

# The Role of Photosensitizer Molecular Charge and Structure on the Efficacy of Photodynamic Therapy against *Leishmania* Parasites

**Oleg E. Akilov,[1,2,4] Sachiko Kosaka,[1,2,4] Katie O'Riordan,[1,2,4] Xiangzhi Song,[3] Margaret Sherwood,[1,2,4] Thomas J. Flotte,[1,2,4] James W. Foley,[3] and Tayyaba Hasan[1,2,4,*]**

[1]Wellman Center for Photomedicine
Massachusetts General Hospital
Boston, Massachusetts 02114
[2]Department of Dermatology
Harvard Medical School
Boston, Massachusetts 02114
[3]The Rowland Institute at Harvard
Cambridge, Massachusetts 02142

## Summary

**Photodynamic therapy (PDT) is emerging as a potential therapeutic modality in the clinical management of cutaneous leishmaniasis (CL). In order to establish a rationale for effective PDT of CL, we investigated the impact of the molecular charge and structure of photosensitizers on the parasitic phototoxic response. Two photosensitizers from the benzophenoxazine family that bear an overall cationic charge and two anionic porphyrinoid molecules were evaluated. The photodynamic activity of the photosensitizers decreases in the following order: EtNBSe > EtNBS > BpD > PpIX. The studies suggest that compared to hydrophobic anionic photosensitizers, the hydrophilic cationic benzophenoxazine analogs provide high effectiveness of PDT possibly due to (1) their strong attraction to the negatively charged parasitic membrane, (2) their hydrophilicity, (3) their high singlet oxygen quantum yield, and (4) their efficacy in targeting intracellular organelles.**

## Introduction

Leishmaniasis, an infectious parasitic disease, is transmitted to humans by the bite of an infected sandfly. Leishmaniasis is endemic in 88 countries, with an estimated yearly incidence of 1–1.5 million cases of cutaneous leishmaniasis (CL) [1]. Despite the various existing antiparasitic medications, the number of cases has not decreased; this is due in part to the high resistance of *Leishmania* to commonly prescribed drugs [2]. The development of an effective, simple, and low-cost treatment that can be administered conveniently is still an active topic of biomedical research in applied parasitology.

Due to current U.S. operations in the Middle East, CL is the focus of considerable interest and investigation. Since January 2003, 853 of the soldiers deployed to southwest Asia have been diagnosed with CL [3]. Clinical observations report an even higher incidence, in approximately 1% of returned troops. While rarely fatal, the ulcerate lesion on the exposed skin can persist for 6–8 months, causing rough scar formation, occasional blood vessel and nerve damage, and secondary infection. This disfigurement and the long duration of the skin lesions present social consequences for the patient.

Very recently, encouraging results with respect to *Leishmania* eradication and low scar formation have been reported with photodynamic therapy (PDT) [4–6]. However, the length of the treatment course (16 weeks) and the lack of sufficient parasitological controls in their reports point to the necessity for a comprehensive study of the potential for PDT in the management of CL. PDT is a photochemistry-based modality where localized light-activated molecules produce toxic molecular species leading to necrosis and/or apoptosis. Various photosensitizers (PSs) have demonstrated light-induced killing activities toward different cell types; however, in dermatologic settings, topical formulations of ALA or its derivates are the most commonly used [7]. While ALA-PDT has been investigated in the management of CL, other photosensitizing molecules not yet explored could be valuable candidates. Porphyrin, chlorin, and phenothiazine molecules demonstrated significant antimicrobial PDT activity in vitro [8], some of which have been used in clinical practice in the treatment of malignancies. The availability of different PSs [9], with various spectra of activity and preferential sites of accumulation, prompted us to establish some guidelines for the optimal photokilling of *Leishmania*.

The hypothesis underlying the current study is based on the observations by many groups [10–12], including ours [13, 14], that PS charge and structure may be important factors in determining the success of antimicrobial PDT, and may also be true for the PDT of CL. Due to the negative surface charge of the *Leishmania* parasite, cationic agents may be more effective than anionic PSs. The overall approach was to evaluate PSs with different charges, including two clinically used porphyrinoid molecules (PpIX and BpD) and two benzophenoxazine analogs (EtNBS and EtNBSe), which have been shown to be effective in oncology [15]. These porphyrinoid compounds were chosen as examples of anionic molecules. The benzophenoxazine analogs, with their highly delocalized positive charge due to the $HN^+$ group, were selected as an example of cationic molecules (Figure 1). In order to more clearly understand the underlying photophysical events, singlet oxygen quantum yields and partition coefficients were evaluated for the benzophenoxazine analogs, but these coefficients are already known for the porphyrins. Experiments evaluating the light-induced killing effect of PpIX were performed in two different ways, ALA-induced PpIX (as reported in clinical studies) and treatment with exogenous PpIX.

## Results

### Comparative Accumulation of Different Photosensitizers by *L. major* Promastigotes

The accumulation of different PSs by *Leishmania major* promastigotes was measured after incubation with

*Correspondence: thasan@partners.org
[4]Lab address: http://www.massgeneral.org/wellman/

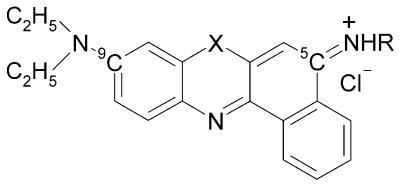

| Dye | X | R | $\lambda_{abs}$(nm)[a] | $\lambda_{fl}$(nm)[a] | $\Phi_{fl}$[a,b] | $^1O_2$[a,c] | Pc[d] |
|---|---|---|---|---|---|---|---|
| NBA | O | H | 623 | 660 | 0.27 | 0.003 | 170 |
| EtNBS | S | $C_2H_5$ | 654 | 693 | 0.21 | 0.03 | 580 |
| EtNBSe | Se | $C_2H_5$ | 661 | 703 | 0.03 | 0.78 | 120 |

a. Measured in methanol containing 0.1% acetic acid at 20°C
b. Absolute fluorescence quantum yield relative to Cresyl Violet (0.55)[26]
c. Absolute quantum yield for singlet oxygen formation relative to Methylene Blue (0.50) [29]
d. Partition coefficient measured in 2-octanol and pH 7.4 buffered saline [15]

Figure 1. Physical and Photochemical Properties of PSs Used in the Study

0.1 μM PS for a 1 hr or 24 hr period. The results of those experiments are presented in Figure 2.

Quantification of intracellular dye accumulation revealed different patterns for different PSs. The lowest level of PS accumulation was established for ALA-induced PpIX ($6.89 \times 10^{-20}$ mol/cell) with an unaltered level 24 hr after incubation ($6.75 \times 10^{-20}$ mol/cell). The initial high accumulation of exogenous PpIX observed within the first hour of incubation was not sustained and gradually decreased after 6 hr of incubation (data not shown). The intracellular concentration of BpD was also low ($5.52 \times 10^{-19}$ mol/cell) and was comparable to the accumulation level of the exogenous PpIX ($p > 0.05$). Accumulation of the benzophenoxazine analogs (EtNBS and EtNBSe) was also determined and revealed that the level of EtNBSe inside the parasite cell was 1.7-fold higher than the intracellular level of BpD and EtNBS after 1 hr of incubation ($p < 0.01$). Thus, EtNBSe showed the highest intracellular accumulation after 1 hr of incubation ($9.39 \times 10^{-19}$ mol/cell) in comparison with the other studied PSs ($p < 0.05$). However, 24 hr after incubation, there were no statistical differences in the level of PSs accumulation in the parasite cells between the PSs (ANOVA, $p > 0.05$).

### Dynamics of Benzophenothiazine Accumulation by *L. major*

To determine the most effective duration for PS incubation, the kinetics of the accumulation of EtNBS and EtNBSe were studied at different time points. The results of the first 2.5 hr are presented in Figure 3. Parasitic cells were incubated for various times at 24°C with 0.1 μM EtNBS or EtNBSe.

In spite of the similar kinetics of the PS accumulation, EtNBSe exhibited higher accumulating ability. The accumulation curves had bell-shaped forms with saturation observed at 1 hr. This was followed by a decrease in the intracellular concentration of PS (40.6% and 46.0% for EtNBSe and EtNBS, respectively) at 2.5 hr. Thus, an hour was the most effective time for exposure of *Leishmania* promastigotes to EtNBS or EtNBSe in vitro.

The kinetics of PpIX and BpD accumulation was also studied (data not shown) and revealed maximum accumulation of PpIX after 6 hr and BpD after 1 hr of coincubation of the PS with *L. major* parasites.

### Photodynamic Killing of *L. major*

The effect of PDT on *Leishmania* cells was studied following 2 hr of incubation of the parasite with different concentrations of PSs. A 2 hr incubation time was chosen in order to allow for the disparity between the accumulation profiles exhibited by different PSs. All irradiations were performed using a fluence of 10 J/cm$^2$. The viability of parasites was determined 18 hr postillumination using the MTT assay to determine cell survival. This method was justified by creating, from three independent experiments, a standard curve correlating cell viability from microscopic enumeration to MTT optical density.

Dark toxicity studies were performed and revealed a PDT effect could be observed at PS concentrations 50- to 100-fold lower than those required for killing of parasites in the absence of light (data not shown). Figure 4 highlights how the treatment of *Leishmania* promastigotes with different PSs exhibited varying phototoxicities. At 18 hr after irradiation, treatment with EtNBS and EtNBSe resulted in more than 90% cell death at concentrations ranging from $1 \times 10^{-6}$ to $1 \times 10^{-7}$ M. However, at the light dose of 10 J/cm$^2$, the half-lethal dose ($LD_{50}$) for EtNBSe was 5.6-fold lower than $LD_{50}$ for EtNBS ($\approx 9.3 \times 10^{-9}$ M versus $\approx 5.2 \times 10^{-8}$ M, respectively). As compared to BpD as the reference PS, EtNBS and EtNBSe were approximately 100- and 500-fold more potent under the present experimental conditions. Exogenous PpIX exhibited phototoxic effects only in very high concentrations ($LD_{50} \approx 3.8 \times 10^{-4}$ M) that probably could not be applied to animal models without serious toxic systemic effects.

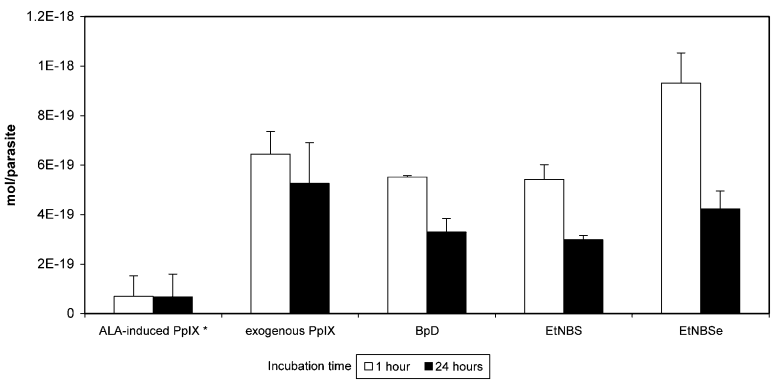


Figure 2. Concentration of PSs per One *L. major* V1 Cell after Incubation with 0.1 μM PS

Each point represents the results of three independent experiments.

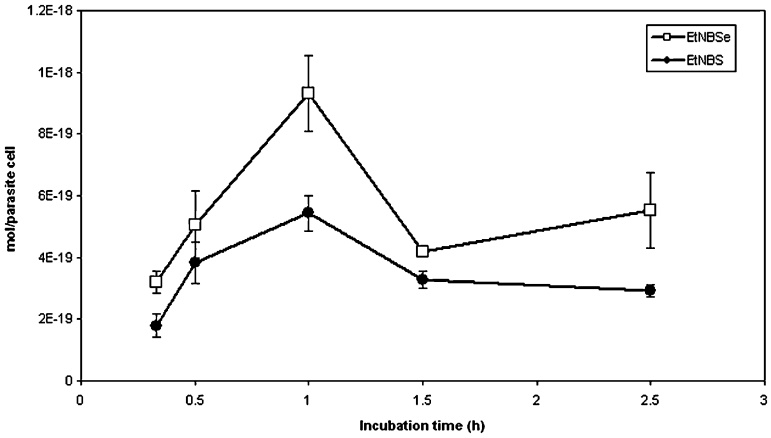


Figure 3. Accumulation Curves of EtNBSe and EtNBS by *L. major* (V1) Promastigotes

PSs (0.1 μM) were added to the cells (2 × $10^7$/ml), and the cellular dye concentrations were determined at different time intervals after incubation at 24°C. Cells were dissolved with 10% SDS and quantification of PS was performed spectrophotometrically. Each point represents the mean ± SD from triplicates.

Interestingly, there was no phototoxicity with ALA-PDT. ALA-PDT not only failed to exhibit any phototoxic activity against the parasites in vitro, but ALA treatment actually increased *Leishmania* survival by 12.3% on average in comparison with the control.

## Physical and Photophysical Properties of EtNBS and EtNBSe

It is generally recognized that to be effective, a PS should absorb electromagnetic radiation in the red or infrared spectrum (the wavelengths of light that penetrate tissue most deeply). It is also desirable that the PS be fluorescent so that it can be located within the targeted species, and thus aid in monitoring PS concentrations. The data presented in Figure 1 indicate that both EtNBS and EtNBSe absorbed red light and were fluorescent. However, because the measurements obtained using PBS rather than methanol revealed $\lambda_{abs}$ = 617 ($\lambda_{fl}$ = 710) for EtNBS and $\lambda_{abs}$ = 620 ($\lambda_{fl}$ = 715) for EtNBSe, for the purpose of PDT on our biological samples we used a 635 nm diode laser as a light source, which corresponds well with this PBS-based absorbance spectra.

EtNBSe exhibited a fluorescence quantum yield 7.0 times smaller than EtNBS, which would make this PS more problematic to trace in biological samples. With respect to singlet oxygen production, the exchange of an oxygen atom for a sulfur or selenium atom significantly increased the singlet oxygen yields (0.03 for EtNBS and 0.78 for EtNBSe) as expected.

Lipophilicity was evaluated for Nile blue A (NBA), EtNBS, and EtNBSe by measuring their partition coefficients using 2-octanol as the oil phase. The data in Figure 1 show that both PSs were quite lipophilic; surprisingly, the selenium analog was significantly less so than the sulfur analog. Nonetheless, when either PS was placed in equal quantities of aqueous and oil phases, visual observation showed the aqueous layer to be colorless, or at most, faintly tinted blue, whereas the oil layer was stained dark blue. In spite of the lipophilic nature of the PSs, they both readily dissolved in isotonic aqueous solutions.

## Light Dose-Dependent Killing Effect of Different PSs against *L. major*

The effectiveness of PDT might be further enhanced by increasing the fluence. We analyzed the results of experiments where parasites were coincubated with PSs at concentrations providing less than 20% of killing in the absence of light and followed that with irradiation performed at different fluences (Figure 5).

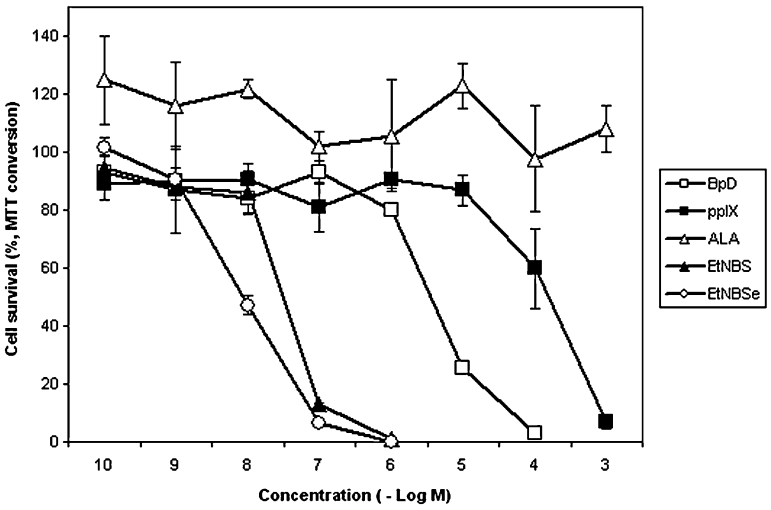


Figure 4. Effect of PDT on *L. major* (V1) Promastigotes In Vitro

Cytotoxic photoactivities of the different PSs toward *L. major* (V1) (18 hr after irradiation). Promastigotes (2 × $10^7$/ml) were incubated with various concentrations (M) of PSs for 2 hr and then light irradiated as described in Experimental Procedures. Cell viability was determined as the percentage of MTT conversion activity. Each point represents the mean ± SD from triplicates.

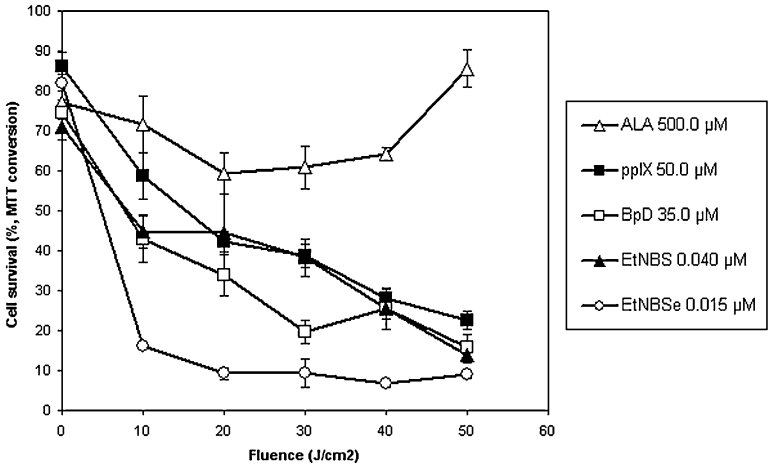


Figure 5. Cytotoxic Photoactivities of the Different PSs toward *L. major* (V1) (18 hr after Irradiation) at Different Fluences

Promastigotes ($2 \times 10^7$/ml) were incubated with $LD_{15–20}$ concentrations (in the absence of light) of PSs for 2 hr and then light irradiated as described in Experimental Procedures. Cell viability was determined as the percentage of MTT conversion activity. Each point represents the mean ± SD from triplicates.

A rate of killing of 77.5%–90.9% after irradiation with a fluence of 50 J/cm$^2$ could be achieved by using different photosensitizing agents except ALA. However, the calculation, based on the overall concentration of PS in the cell suspension, demonstrated that $1.06 \times 10^9$ molecules of EtNBSe were required for killing one parasite at 50 J/cm$^2$ in comparison with $5.70 \times 10^9$ molecules of EtNBS, $4.38 \times 10^{12}$ molecules of BpD, and $1.67 \times 10^{13}$ molecules of exogenous PpIX. In addition, a good phototoxic effect (84.0% of parasites were eliminated) was achieved in the case of EtNBSe at fluences as low as 10 J/cm$^2$, while EtNBS required 30 J/cm$^2$ to kill 80.4% of the parasites.

The ineffectiveness of ALA was further demonstrated by the observation that the phototoxicity did not exceed 40% even at a fluence of 30–50 J/cm$^2$.

### Pathomorphological Changes in *L. major* Promastigotes after BpD- or EtNBSe-PDT

Morphological changes in *Leishmania* parasites exposed to EtNBSe and BpD were studied to determine the subcellular impact of two different PDT treatments.

The normal morphology of metacyclic promastigotes (4 days cultivation) is presented in Figure 6a (light microscopy) and Figure 6A (transmission electron microscopy; TEM). *Leishmania* parasites appeared characteristically pear-shaped with blue (Quik-Dip staining) cytoplasm, a prominent round red (Quik-Dip) nucleus in the center of the cell, and an apically located kinetoplast, also stained red due to DNA contents. TEM of the normal structure of the *L. major* metacyclic promastigote without treatment (control) is presented in Figure 6A. Ultrastructural characteristics typical for members of the *Trypanosomatidae* family can be seen in this figure: the elongated shape of the parasitic cell with a single nucleus (N). The nucleus has two perforated membranes (nuclear envelope) and possesses a prominent nucleolus (no) positioned centrally; the chromatin is arranged peripherally. In the apical part of the parasite cell, a flagellum (F) originates from the basal body apparatus (b). A kinetoplast (k) lies posteriorly to the basal body and contains a fibrous k-DNA disc. The longitudinal section (right lower corner of Figure 6A), showing the kinetoplast (k), gives rise to a single mitochondrial ramus (m), which extends posteriorly past an elongated nucleus. Ultrastructural analysis also revealed the presence within the cytoplasm of membrane-associated organelles such as a Golgi apparatus (g) and a variety of membrane-bound vacuoles (inclusion vacuoles, iv).

The PDT regimes were selected in such a way that they provide only a 50% killing effect and thus enabled us to monitor viable and dead cells. For that reason, parasites were exposed to 15 nM EtNBSe and 35 μM BpD and were irradiated at the same fluence (10 J/cm$^2$).

Comparative analysis of immersion light microscopy and TEM revealed characteristic morphological changes in the ultrastructure of parasite cells. These changes were dependent on the particular PS to which they were exposed (Figure 6). As shown in the photographs from the light microscopy 6 hr after BpD-PDT, the width of parasites decreased approximately by half in comparison with the controls (Figure 6b). The cytoplasm lost its usual blue color (Quik-Dip) and appeared light purple, while the nucleus remained unchanged and centrally positioned. On the corresponding TEM photos (Figure 6B), the following features can be seen: during the sublethal damage, the most prominent feature was a swelling of the mitochondrion, sometimes accompanied by the destruction of the mitochondrial membrane and the leakage of internal contents into the cytoplasm. Dead cells exhibited chaotic disorganization of their cytoplasm, although the nucleus remained inside the cell.

Different changes were found after EtNBSe-PDT (Figures 6c and 6C). As early as 1 hr after EtNBSe-PDT, changes in the morphology of the parasites could be observed. Cells changed from their characteristic elongated shape into a rounded form. Parasites appeared swollen. Cellular cytoplasm lost its usual blue color (Quik-Dip) and appeared light purple. The volume of the nuclei increased to twice their normal size. Most of the nuclei lost their usual compact round shape. Leakage to the cytoplasm and fenestration of the nuclear materials were observed (Figure 6c). TEM supported those findings and also revealed details of nuclear alteration, which consisted of damage to the nuclear envelope, condensation of nuclear material, and final confluence with cytoplasm. Consistent swelling of the kinetoplast was also observed (Figure 6C).

More dramatic changes were observed 24 hr after PDT (Figures 6d and 6D). Cells after BpD-PDT showed secondary swelling. Their cytoplasm contained lipid

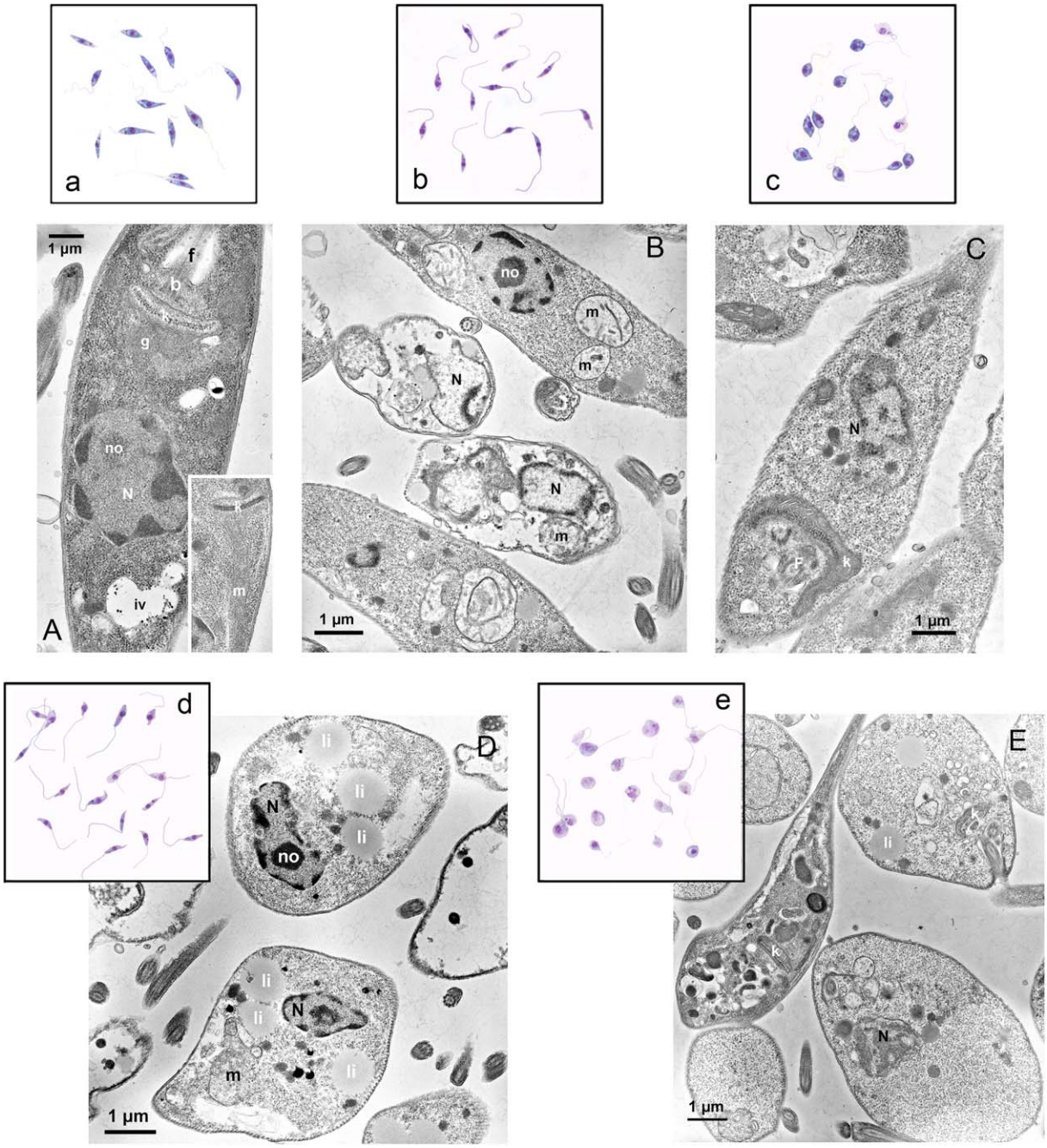


Figure 6. Ultrastructural Changes in the Morphology of *Leishmania* Promastigotes during BpD-PDT and EtNBSe-PDT

Promastigotes ($2 \times 10^7$) were incubated with 15 nM EtNBSe or 35 μM BpD for 1 hr and then were irradiated with 635 nm (in the case of EtNBSe) or 690 nm (in the case of BpD) diode laser to a fluence of 10 J/cm$^2$. For light microscopy, cytospin samples were stained with Quik-Dip and photos were made at ×1500 (a–e). For TEM, parasites were fixed at 6 hr (B and C) or 24 hr (D and E) after PDT. The morphology of unexposed *Leishmania* promastigotes presented as a control (a and A). Damage of the cytoplasm is a leading cause of death 6 hr after BpD-PDT (b and B), while disorganization of the nucleus and gradually swelling of the parasitic cell are the major changes 6 hr after EtNBSe-PDT (c and C). Secondary swelling of dead parasitic cells with destroyed cytoplasm 24 hr after BpD-PDT (d and D). Degenerative changes with lipid accumulation 24 hr after EtNBSe-PDT (e and E). N, nucleus; b, basal body apparatus; g, Golgi apparatus; f, flagellum; k, kinetoplast; r, reservoir; m, mitochondrion; no, nucleolus; iv, inclusion vacuole; li, lipid body.

inclusions as a marker of lipodystrophy. However, the nucleus could still be observed in most of the cells (Figure 6D). Parasites after EtNBSe-PDT also were swollen with a variety of vacuoles (autolysosomes were the most frequent type of vacuoles in this case). Nuclei in most of the cells disappeared, although nuclear material sometimes could be found in the cytoplasm as a scanty chromatin condensate. The edematous kinetoplast could occupy as much as one fifth to one third of the volume of the cell (Figure 6E).

Thus, the mechanism of BpD-PDT was a primary disorganization of the cytoplasm with parallel mitochondrion

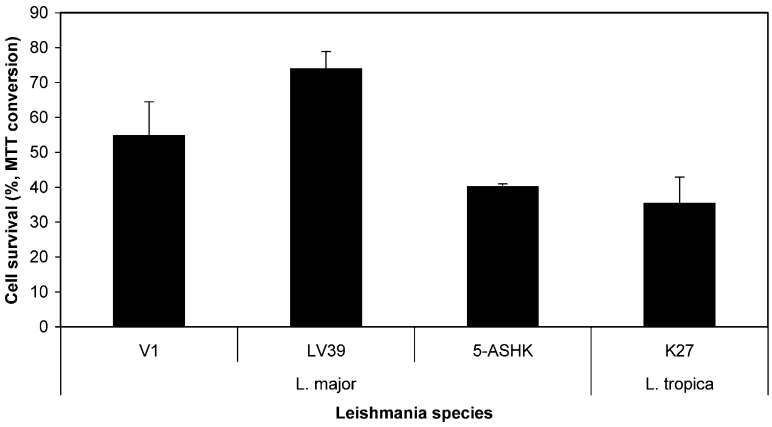


Figure 7. Phototoxic Activities of EtNBSe toward Different Skin-Tropic Strains of *Leishmania*

Promastigotes ($2.0 \times 10^7$) were incubated with 0.1 μM EtNBSe and irradiated after 1 hr of incubation with a 635 nm diode laser to a fluence of 10 J/cm$^2$.

alteration, while the mechanism of EtNBSe-PDT was a primary damage of the nuclear membrane with resulting leakage of the nuclear material into the cytoplasm.

### Phototoxic Activity of EtNBSe toward Different Skin-Tropic Strains of *Leishmania*

To establish the effectiveness of proposed PDT regimes, we compared phototoxic activity of EtNBSe toward different skin-tropic strains of *Leishmania* parasites. For this purpose, $2.0 \times 10^7$ promastigotes of different *Leishmania* strains were incubated with 0.1 μM EtNBSe and irradiated after 1 hr incubation with a 635 nm diode laser at a fluence of 10 J/cm$^2$ (Figure 7).

While 54.8 ± 9.6% of *L. major* V1 survived 1 hr after EtNBSe-PDT, LV39 exhibited lower sensitivity, showing 74.0 ± 4.9% of viability of exposed cells. The strains of *L. major* from Ashgabad (5-ASKH) and *L. tropica* K27 showed similar low survival ability (40.1 ± 0.8% and 35.4 ± 7.6%, respectively). Thus, EtNBSe is a substantially effective and promising photosensitizing agent against skin-tropic strains of *Leishmania*.

## Discussion

This report is among the first to compare the phototoxicities of different classes of PSs against *Leishmania* parasites with a specific focus on the zoonotic skin-tropic strain *Leishmania major*. In addition to molecular charge, singlet oxygen quantum yield and the partition coefficient were evaluated as possible parameters governing PDT efficacy. The study demonstrated that when compared to hydrophobic anionic PSs, the cationic benzophenoxazine analogs have a stronger binding interaction with the negatively charged membrane of the parasite and the high singlet oxygen quantum yield. In the case of the benzophenoxazine analogs, greater PDT effectiveness may be due to the intracellular sites that they target.

Different PSs exhibited different accumulation patterns, with the lowest level in the case of ALA-induced PpIX. The low accumulation of ALA can be explained by the particular features of porphyrin biosynthesis in the *Leishmania* organism [16]. As *Leishmania* parasites are deficient in the enzymes required for heme biosynthesis, ALA cannot be utilized as a source for hemin or PpIX. Parasites manifest a nutritional demand for hemin and PpIX [17]. Thus, the low permanent reading in the case of ALA-induced PpIX is probably from background autofluorescence.

Our results indicate that the levels of intracellular accumulation of the benzophenoxazine analogs and two anionic porphyrinoid molecules were comparable. The cationic molecules still exhibited the highest phototoxic activity toward *Leishmania* parasites, highlighting the importance of the charge interaction between the anionic parasitic membrane and the delocalized cationic charge of benzophenothiazines. EtNBS and EtNBSe are relatively small, planar rigid structures that harbor a delocalized cationic charge that can be neutralized by the removal of a proton from the C-5 amino group [15]. One of the major components of the external surface of *Leishmania* parasites responsible for the membrane surface charge is lipophosphoglycan (LPG). LPG is a polymer of phosphorylated disaccharide repeat units attached by a polysaccharide core to a novel lipid anchor. Several reports have confirmed this role for LPG in conferring a negative charge to the surface of *Leishmania* [18–20].

The exchange of an oxygen atom for a sulfur or selenium atom in benzophenoxazine analogs significantly increases the singlet oxygen yields, in turn leading to high phototoxic activity. PSs usually inactivate biological targets via their excited triplet states. This occurs primarily because the millisecond lifetimes of this species are long enough to participate in bimolecular chemistry, whereas the nanosecond lifetimes of the corresponding excited singlet state generally preclude this behavior. A PS can inactivate targets in one of two ways: (1) via an electron transfer reaction directly with the target or with some other species to produce cytotoxic radicals, or (2) via transfer of its electronic energy to ground state oxygen, generating highly cytotoxic $^1O_2$, with regeneration of the PS [21]. Regardless of which mechanism a PDT agent employs, an efficient PS must give a high triplet quantum yield. Because it is well established that in aerated alcoholic solvents, triplet states of phenothiazine PSs (such as those studied herein) generate singlet oxygen with 100% efficiencies due to their π-π character, we chose to determine the triplet quantum yields of EtNBS and EtNBSe indirectly by measuring singlet oxygen quantum yields. As the incorporation of a heavy atom into a molecule with a low intrinsic

intersystem cross rate constant will increase the probability of such a transition, it was determined that replacing the central oxygen atom with a somewhat heavier sulfur atom resulted in a small but significant increase in the triplet yield; replacement of the oxygen atom by a much heavier selenium atom resulted in a dramatic improvement in the triplet yield. This biophysical property has a direct relation to PDT efficacy: the number of molecules of EtNBSe required for killing one parasite at 50 J/cm$^2$ was 5.7 times lower when compared to the number of molecules of EtNBS needed.

The $^1O_2$ quantum yield of EtNBSe and BpD was the same, equal to 0.78 [22], indicating possibly other critical factors in PDT efficacy, such as PS penetration and the site of accumulation inside the target cell. Lipophilicity is often found to be an important predictor for PS accumulation in mammalian cells [23]. Comparison of the partition coefficient of benzophenoxazine analogs with BpD revealed that the anionic porphyrinoid molecule was 750 times more lipophilic than EtNBSe (partition coefficient for BpD was 90,000, as cited in [23]). The decreasing lipophilicity of the compounds studied can be presented in the following order: BpD > PpIX > EtNBS > EtNBSe. Our experiments revealed that the effectiveness of PSs correlated with the partition coefficient, and was therefore, inversely proportional to lipophilicity. The photodynamic activity of the PS increased in the following order: PpIX < BpD < EtNBS < EtNBSe. The alteration of this order in the case of BpD and PpIX [24] could be explained by the higher $^1O_2$ quantum yield of BpD. The data strongly suggest that in addition to photophysical properties, parameters such as hydrophilicity/lipophilicity play a fundamental role in the improvement of photokilling efficacy.

As was demonstrated in the murine model of a solid tumor, the predominant accumulation of EtNBS/EtNBSe occurred in lysosomes, with a subsequent release of lysosomal enzymes and autophagia of the host cells following irradiation [15]. In our study, data obtained by TEM accentuated nuclear membrane damage as the major mechanism of parasite death. It also appears that damage to the cytoplasm occurred. The prominent swelling of parasites was evidence of the disturbance of the water-electrolytic balance, which is regulated by cytoplasmic pumps. In comparison to BpD, which affected primarily mitochondrial and intracytoplasmic structures, the changes from the benzophenoxazine analogs were more drastic, due to the effective destruction of the nuclear membrane. Thus, taking into account the comparable level of $^1O_2$ quantum yield of EtNBSe and BpD, the intracellular site of photosensitization appears to be critical.

## Significance

**The results of our study show that the positively charged benzophenoxazine analogs, and in particular, EtNBSe, are promising PSs against skin-tropic strains of *Leishmania*. EtNBSe provides an efficient killing effect in a concentration as low as $1.06 \times 10^9$ molecules per parasite. For the broader significance of these data, future investigations must monitor PDT efficacy using an in vivo model of the disease. In tissue, *Leishmania* parasites are located predominantly intracellularly. Therefore, the direct effect of PDT could destroy both parasites and infected cells. PSs that selectively accumulate inside the parasite, allowing destruction of the parasite without damage to the host cell, are not presently available.**

## Experimental Procedures

### Chemicals

δ-aminolevulinic acid (ALA; purity ~98%) and protoporphyrin IX (PpIX; purity ~95%) were purchased from Sigma-Aldrich (St. Louis, MO). 5-ethylamino-9-diethylaminobenzo[*a*]phenothiazinium chloride (EtNBS) was synthesized according to procedures described in U.S. patent 4,962,197. General synthetic schemes for 5-ethylamino-9-diethylaminobenzo[*a*]phenoselenazinium chloride (EtNBSe) are well documented [25]. EtNBS and EtNBSe dyes were purified by medium pressure (100 psi) liquid chromatography (purity ~90%–95%). The benzoporphyrin derivative (BpD; purity ~99.9%) was a generous gift of QLT PhotoTherapeutics (Vancouver, Canada). The compound was stored at −70°C in dimethyl sulfoxide. It was diluted in Hank's media + 10% fetal calf serum (FCS), and the concentration was determined spectrophotometrically ($\varepsilon_{690}$ = 31,200) before each use.

### Fluorescence Quantum Yields

Fluorescence quantum yields for EtNBS and EtNBSe were determined spectrophotometrically relative to a known standard at 20°C in methanol acidified with 0.1% acetic acid to ensure that the PS remained in their cationic states throughout the measurement. Typically, the optical density (OD) of each contained in a thermostated cuvette was adjusted to OD = 0.050 at 600 nm. The excitation wavelength of the spectrofluorometer was set to 600 nm and kept static throughout all experiments. The integrated intensity of the corrected emission spectrum obtained for each dye was compared to the value recorded for cresyl violet, which has an absolute quantum yield of 0.54 in methanol [26]. Reported values are the average of three measurements with an estimated accuracy of ±5% that result from systematic errors inherent in the method [27].

### The Quantum Yield for $^1O_2$ Formation

The quantum yield for $^1O_2$ formation for the benzophenoxazine analogs was determined by measuring the $^1O_2$-mediated bleaching of 1,3-diphenylisobenzofuran [28]. A cuvette containing a mechanically stirred methanol solution of the dye (OD at 632.8 nm = 1.000) and furan $^1O_2$ receptor (OD = 0.900 at 410 nm) was illuminated with an expanded beam (ca. 5 mm diameter) of a stabilized HeNe laser (0.5 mW, 632.8 nm). The HeNe beam was absorbed only by the PS. The rate of furan bleaching by reaction with $^1O_2$ was measured spectrophotometrically by the disappearance of the 410 nm band as a function of time. Singlet oxygen yields for each dye were calculated by comparing their rates to that measured for methylene blue, whose absolute $^1O_2$ quantum yield is 0.50 [29]. Determinations of $^1O_2$ yields were performed three times for each dye.

### Partition Coefficients

Partition coefficients were determined according to the procedure previously reported [15]. Briefly, a known amount of dye was shaken for 5 min in a solvent system consisting of measured volumes of phosphate-buffered saline and 2-octanol. After allowing the mixture to remain quiescent for 30 min, the amount of dye residing in the 2-octanol layer was measured spectrophotometrically. The volume and concentration measurements were used to calculate the partition coefficient using a standard equation [30].

### Parasites

The following *Leishmania* strains were used in this study: *L. major* NIH Friedlin V1 strain (MHOM/IL/80/FN), isolated from a patient with localized CL in Israel; *L. major* LV39 (MRHO/SU/59/P), isolated from a gerbil reservoir in southern Russia; *L. major* World Health Organization reference strain 5-ASKH (MHOM/SU/73/5-ASKH), a human cutaneous isolate from Turkmenistan; *L. tropica* K27 (MHOM/SU/74/K27), isolated from a patient with a cutaneous lesion in Azerbaijan. V1 and LV39 were generous gifts from Dr. Mary Ann

McDowell (Department of Biological Science, University of Notre Dame, Notre Dame, IN), and 5-ASKH and K27 were purchased from American Type Culture Collection (Rockville, MD). All *Leishmania* parasites were cultured at 24°C without $CO_2$ in medium 199 (M199) supplemented with 20% heat-inactivated FCS, 60 ng/ml penicillin G sodium salt, 100 ng/ml kanamycin sulfate, 50 ng/ml flucytosine, 10 ng/ml chloramphenicol, 2 mM L-glutamine, 40 mM HEPES, 0.1 mM adenine (in 50 mM HEPES), 5 mg/ml hemin (in 50% triethanolamine), and 1 mg/ml 6-biotin (medium 199 complete; M199-C).

A concern exists about using intracellular parasites in experiments due to their higher relevance to potential therapy. For research purposes, amastigotes could be obtained either from short-term in vitro cultivation in murine peritoneal macrophages or other macrophage cell lines (see [31] for references to original reports), or from infected tissues [32]. However, these preparations are frequently contaminated with adsorbed host components so that studies using them (e.g., models of infection in vivo, immunological studies) can be misleading. Studies with *Leishmania mexicana* have demonstrated the possibility of amastigote generation under specific temperature conditions [33]. Our observations indicate that amastigotes of *L. major* obtained under similar conditions as *L. amazonensis* are unstable and transform to the procyclic organism in 2 hr (data not shown). Thus, it is impossible to use *L. major* amastigotes for the purpose of assessing PDT efficacy, and promastigotes were used in the study. Infective-stage metacyclic promastigotes were isolated from stationary cultures (4–5 days old) by using a uniform procedure based on the modification of a density gradient purification [34].

### Cytospin Preparations

Cytospins were prepared using a Shandon Cytospin 4 cytocentrifuge (Shandon Lipshaw, Pittsburgh, PA) set at 600 rpm for 10 min. After Quik-Dip staining (Mercedes Medical, Sarasota, FL), light microscopic analysis of the cells was performed on an Axiophot microscope (Zeiss, West Germany).

### Photosensitizer Accumulation Assay

Infective-stage metacyclic promastigotes ($2 \times 10^7$) were incubated for 1 or 24 hr with 0.1 μM PS in M199-C and then were washed twice with PBS. Parasites were solubilized in 1 ml 10% aqueous solution of sodium dodecyl sulfate (SDS). The fluorescence of the cell lysate was read in a microplate spectrophotometer (SPECTRAmax GEMINI EM, Molecular Devices, Sunnyvale, CA), using a serial dilution of PS as a standard curve. The standards of PSs were also prepared in a 10% aqueous solution of SDS. SDS was used as an osmotic and chemical disruptor of cellular membranes, facilitating the release of the cellular contents. Solubilization of products was sufficient enough not to use additional solvents such as DMSO and acidic isopropanol. In parallel, after incubation with PS, the number of viable parasites in a sample was determined in an MTT assay. The concentration of PS per parasite cell was established as a division of concentration of PS per number of parasites in a sample.

### Photodynamic Therapy

Metacyclic promastigotes were incubated for 1 hr in darkness with PS in M199-C at 24°C. Cells were transferred to a 35 mm Petri dish and then exposed to a light source (HPD diode laser source model 7401, High Power Devices, North Brunswick, NJ) with a wavelength of 635 nm for ALA, PpIX, EtNBS, and EtNBSe, and 690 nm for BpD. The fluorescence intensity was measured by a Lasermate/D power meter (Coherent, Santa Clara, CA). Following irradiation of the cells, 2 ml of fresh growth medium was added. After 18 hr, an MTT assay was performed to determine cell survival. Each experiment included three controls: unexposed parasites without treatment, cells treated with a dye but not exposed to light, and cells exposed to light but not treated with a dye.

### MTT Assay

The relative number of viable *Leishmania* was determined as described previously [35–37]. The MTT assay was selected because it allows the determination of viable cells. Briefly, the parasite suspension was centrifuged 10 min at 3500 rpm and the supernatant was poured off. Cells were resuspended in 200 μl MTT solution (10 mg/ml 3-[4,5-dimethylthiazol-2-yl]-2,5-diphenyltetrazolium bromide in PBS with 3% FCS). After incubation at 24°C for 40 min and washing with PBS, the pellet was dissolved in 10% aqueous solution of SDS. MTT cleavage was measured on a microplate spectrophotometer (SPECTRAmax 340 PC, Molecular Devices) using a test wavelength of 560 nm. Correlation between the MTT cleavage reading and the number of parasites was established in the standard curve.

### Transmission Electron Microscopy

Control and treated promastigotes of *L. major* NIH Friedlin V1 strain were fixed in 2.5% glutaraldehyde + 2% paraformaldehyde overnight at 4°C. After spinning down (1200 rpm) and decanting the fixative, 0.1 M sodium cacodylate buffer (pH 7.2) was added to the pellets. After fixation, hot agar (2% in distilled water, heated to boiling) was immediately added to each pellet. Once the agar had hardened, the cell pellets were then processed routinely, as any other tissue, for TEM. The cell pellets were postfixed in 2% $OsO_4$ in sodium cacodylate buffer, dehydrated in a graded alcohol series, and embedded in Epon t812 (Tousimis, Rockville, MD). Ultrathin sections were cut on a Reichert-Jung Ultracut E microtome (Vienna, Austria), collected on uncoated 200 mesh copper grids, stained with uranyl acetate and lead citrate, and examined on a Philips CM-10 transmission electron microscope (Eindhoven, The Netherlands). The negatives were scanned on an Epson Perfection 3200 photoscanner. Multiple parasite sections were microscopically analyzed and images representing the most typically observed morphologies were prepared for the Results.

### Statistical Analyses

The statistical analysis was based on the calculation of arithmetic mean and standard deviation. One-way ANOVA was used for group comparison. Bonferroni's multiple comparison test was chosen when certain pairs had to be analyzed. A p value of less than 0.05 was considered statistically significant.

### Acknowledgments

We are grateful to Dr. Mary Ann McDowell (Department of Biological Science, University of Notre Dame, Notre Dame, IN) for providing us the *L. major* strain V1 and strain LV39. We are appreciative of Elizabeth Davis for excellent assistance with our manuscript preparation. This work was funded by Medical Free Electron Laser Program grant FA9550-04-1-0079 from the Department of Defense (to T.H.).

Received: January 31, 2006
Revised: June 2, 2006
Accepted: June 7, 2006
Published: August 25, 2006

### References

1. Desjeux, P. (2004). Leishmaniasis: current situation and new perspectives. Comp. Immunol. Microbiol. Infect. Dis. *27*, 305–318.
2. Ouellette, M., Drummelsmith, J., and Papadopoulou, B. (2004). Leishmaniasis: drugs in the clinic, resistance and new developments. Drug Resist. Updat. *7*, 257–266.
3. Repaci, P. (2006). Leishmaniasis and other parasitic diseases among OIF/OEF soldiers. (http://www.pdhealth.mil/downloads/OTSGLeishmaniasisInformationPaper29Mar06_24042006.pdf).
4. Gardlo, K., Horska, Z., Enk, C.D., Rauch, L., Megahed, M., Ruzicka, T., and Fritsch, C. (2003). Treatment of cutaneous leishmaniasis by photodynamic therapy. J. Am. Acad. Dermatol. *48*, 893–896.
5. Gardlo, K., Hanneken, S., Ruzicka, T., and Neumann, N.J. (2004). Photodynamic therapy of cutaneous leishmaniasis. A promising new therapeutic modality, in German. Hautarzt *55*, 381–383.
6. Enk, C.D., Fritsch, C., Jonas, F., Nasereddin, A., Ingber, A., Jaffe, C.L., and Ruzicka, T. (2003). Treatment of cutaneous leishmaniasis with photodynamic therapy. Arch. Dermatol. *139*, 432–434.
7. Kelty, C.J., Brown, N.J., Reed, M.W., and Ackroyd, R. (2002). The use of 5-aminolaevulinic acid as a photosensitiser in photodynamic therapy and photodiagnosis. Photochem. Photobiol. Sci. *1*, 158–168.

8. Brown, S.B. (2005). Antimicrobial PDT: we have heard the theory, what about the practice? In The 11th Congress of the European Society for Photobiology, J. Piette, ed. (Pisa: Institute of Informatics and Telematics), pp. 100–101.
9. Dutta, S., Ray, D., Kolli, B.K., and Chang, K.P. (2005). Photodynamic sensitization of *Leishmania amazonensis* in both extracellular and intracellular stages with aluminum phthalocyanine chloride for photolysis in vitro. Antimicrob. Agents Chemother. *49*, 4474–4484.
10. Bremner, J.C., Wood, S.R., Bradley, J.K., Griffiths, J., Adams, G.E., and Brown, S.B. (1999). 31P magnetic resonance spectroscopy as a predictor of efficacy in photodynamic therapy using differently charged zinc phthalocyanines. Br. J. Cancer *81*, 616–621.
11. Ball, D.J., Mayhew, S., Wood, S.R., Griffiths, J., Vernon, D.I., and Brown, S.B. (1999). A comparative study of the cellular uptake and photodynamic efficacy of three novel zinc phthalocyanines of differing charge. Photochem. Photobiol. *69*, 390–396.
12. Villanueva, A., and Jori, G. (1993). Pharmacokinetic and tumour-photosensitizing properties of the cationic porphyrin meso-tetra(4N-methylpyridyl)porphine. Cancer Lett. *73*, 59–64.
13. Soukos, N.S., Ximenez-Fyvie, L.A., Hamblin, M.R., Socransky, S.S., and Hasan, T. (1998). Targeted antimicrobial photochemotherapy. Antimicrob. Agents Chemother. *42*, 2595–2601.
14. Hamblin, M.R., and Hasan, T. (2004). Photodynamic therapy: a new antimicrobial approach to infectious disease? Photochem. Photobiol. Sci. *3*, 436–450.
15. Cincotta, L., Foley, J.W., and Cincotta, A.H. (1993). Phototoxicity, redox behavior, and pharmacokinetics of benzophenoxazine analogues in EMT-6 murine sarcoma cells. Cancer Res. *53*, 2571–2580.
16. Sah, J.F., Ito, H., Kolli, B.K., Peterson, D.A., Sassa, S., and Chang, K.P. (2002). Genetic rescue of *Leishmania* deficiency in porphyrin biosynthesis creates mutants suitable for analysis of cellular events in uroporphyria and for photodynamic therapy. J. Biol. Chem. *277*, 14902–14909.
17. Chang, C.S., and Chang, K.P. (1985). Heme requirement and acquisition by extracellular and intracellular stages of *Leishmania mexicana amazonensis*. Mol. Biochem. Parasitol. *16*, 267–276.
18. Silva Filho, F.C., Saraiva, E.M., Santos, M.A., and de Souza, W. (1990). The surface free energy of *Leishmania mexicana amazonensis*. Cell Biophys. *17*, 137–151.
19. Handman, E., and Goding, J.W. (1985). The *Leishmania* receptor for macrophages is a lipid-containing glycoconjugate. EMBO J. *4*, 329–336.
20. Turco, S.J. (1988). The lipophosphoglycan of *Leishmania*. Parasitol. Today *4*, 255–257.
21. W.M. Horspool and P.-S. Song, eds. (1994). CRC Handbook of Organic Photochemistry and Photobiology (Boca Raton, FL: CRC Press).
22. Aveline, B., Hasan, T., and Redmond, R.W. (1994). Photophysical and photosensitizing properties of benzoporphyrin derivative monoacid ring A (BPD-MA). Photochem. Photobiol. *59*, 328–335.
23. Okunaka, T., Eckhauser, M.L., Kato, H., Bomaminio, A., Yamamoto, H., Aizawa, K., Sarasua, M.M., and Koehler, K.A. (1992). Correlation between photodynamic efficacy of differing porphyrins and membrane partitioning behavior. Lasers Surg. Med. *12*, 98–103.
24. Georgakoudi, I., and Foster, T.H. (1998). Singlet oxygen- versus nonsinglet oxygen-mediated mechanisms of sensitizer photobleaching and their effects on photodynamic dosimetry. Photochem. Photobiol. *67*, 612–625.
25. Groves, J.T., Lindenauer, S.M., Haywood, B.J., Knol, J.A., and Schultz, J.S. (1974). Synthesis of seleno-toluidine blue. J. Med. Chem. *17*, 902–904.
26. Magde, D., Brannon, J.H., Cremers, T.L., and Olmsted, J.I. (1979). Absolute luminescence yield of cresyl violet. A standard for the red. J. Phys. Chem. *83*, 696–699.
27. Magde, D., Wong, R., and Seybold, P.G. (2002). Fluorescence quantum yields and their relation to lifetimes of rhodamine 6G and fluorescein in nine solvents: improved absolute standards for quantum yields. Photochem. Photobiol. *75*, 327–334.
28. Cincotta, L., Foley, J.W., and Cincotta, A.H. (1987). Novel red absorbing benzo[a]phenoxazinium and benzo[a]phenothiazinium photosensitizers: in vitro evaluation. Photochem. Photobiol. *46*, 751–758.
29. Tanielian, C., Wolff, C., and Esch, M. (1996). Singlet oxygen production in water: aggregation and charge-transfer effects. J. Phys. Chem. *100*, 6555–6560.
30. Pooler, J.P., and Valenzeno, D.P. (1979). Physicochemical determinants of the sensitizing effectiveness for photooxidation of nerve membranes by fluorescein derivatives. Photochem. Photobiol. *30*, 491–498.
31. Bates, P.A., Robertson, C.D., Tetley, L., and Coombs, G.H. (1992). Axenic cultivation and characterization of *Leishmania mexicana* amastigote-like forms. Parasitology *105*, 193–202.
32. Glaser, T.A., Wells, S.J., Spithill, T.W., Pettitt, J.M., Humphris, D.C., and Mukkada, A.J. (1990). *Leishmania major* and *L. donovani*: a method for rapid purification of amastigotes. Exp. Parasitol. *71*, 343–345.
33. Peters, C., Aebischer, T., Stierhof, Y.D., Fuchs, M., and Overath, P. (1995). The role of macrophage receptors in adhesion and uptake of *Leishmania mexicana* amastigotes. J. Cell Sci. *108*, 3715–3724.
34. Spath, G.F., and Beverley, S.M. (2001). A lipophosphoglycan-independent method for isolation of infective *Leishmania* metacyclic promastigotes by density gradient centrifugation. Exp. Parasitol. *99*, 97–103.
35. Taleb-Contini, S.H., Salvador, M.J., Balanco, J.M., Albuquerque, S., and de Oliveira, D.C. (2004). Antiprotozoal effect of crude extracts and flavonoids isolated from *Chromolaena hirsuta* (asteraceae). Phytother. Res. *18*, 250–254.
36. Moreira, M.E., Del Portillo, H.A., Milder, R.V., Balanco, J.M., and Barcinski, M.A. (1996). Heat shock induction of apoptosis in promastigotes of the unicellular organism *Leishmania* (*Leishmania*) *amazonensis*. J. Cell. Physiol. *167*, 305–313.
37. Kiderlen, A.F., and Kaye, P.M. (1990). A modified colorimetric assay of macrophage activation for intracellular cytotoxicity against *Leishmania* parasites. J. Immunol. Methods *127*, 11–18.